Hindawi
International Journal of Aerospace Engineering
Volume 2019, Article ID 7851260, 7 pages
https://doi.org/10.1155/2019/7851260

Research Article

Structural Parameter Sensitivity Analysis of an Aircraft Anti-Icing Cavity Based on Thermal Efficiency

Feng Zhang [1], **Yang Gao** [1], **Huiju Yao** [2], **Yameng Wang** [1], **and Kailiang Luo** [1]

[1] *School of Mechanics, Civil Engineering and Architecture, Northwestern Polytechnical University, Xi'an 710129, China*
[2] *Jiangnan Institute of Electrical and Mechanical Design, Guiyang 550009, China*

Correspondence should be addressed to Feng Zhang; nwpuwindy@nwpu.edu.cn

Received 12 July 2018; Revised 30 November 2018; Accepted 24 December 2018; Published 28 February 2019

Academic Editor: Jose Carlos Páscoa

The objective of this paper is to accurately describe the influence of structural parameter uncertainties on the thermal efficiency of an aircraft wing anti-icing cavity. To do this, a new method of parameter sensitivity evaluation is proposed according to the weighted stochastic response surface method. First, the concept of fitting the explicit performance function of the anti-icing cavity structure using the weighted stochastic response surface method is presented. A structural parameter sensitivity analysis based on thermal efficiency is then conducted considering the uncertainties of the position of the flute tube, the height of the double-skin channel, and the diameter and angle of the jet holes. The results indicate that the height of the double-skin channel and the diameter of the jet holes are the main factors influencing the functional reliability of the anti-icing cavity.

1. Introduction

Ice accretion on airfoils can cause significant damage to an aircraft not only by increasing its weight but also by deteriorating its aerodynamic capabilities and decreasing the available lift force, affecting its stability and safe operation [1–4]. Most modern aircraft in operation today, such as the Airbus 320 or Boeing 747, employ a thermal anti-icing system as the main deicing and anti-icing method.

With the development of large aircraft projects in China, the study of airfoil thermal anti-icing systems has attracted increasing attention. As the core part of an airfoil thermal anti-icing system, the design quality of the anti-icing cavity has a significant impact on the deicing and anti-icing effect provided to the aircraft [5, 6]. Parameters such as the jet hole angle, jet hole diameter, and distance between the jet holes and aircraft skin anti-icing area should be adjusted so that the air supply system can effectively provide sufficient hot air for deicing [7–10]. Traditional studies on anti-icing systems have mainly focused on the simulation of the flow characteristics inside the cavity and the heat exchange between the cavity and the aircraft skin under the condition that the geometric structure of the anti-icing cavity is well known. Under this approach, the anti-icing surface temperature can be obtained by calculating the coupled results of the flow and heat transfer equations without considering the influence of structural parameter uncertainty on the anti-icing performance [8, 9].

When considering error factors introduced by manufacture and assembly, the actual dimensions of the anti-icing cavity will inherently have a certain degree of uncertainty [7]. Thus, although the properties of an anti-icing cavity can be determined during an anti-icing property experiment, its functionality could still fail to be up to standard in practical use. Reliability sensitivity [11–14] can accordingly be used to analyse the influence of anti-icing cavity structure parameters on functional reliability and is instructive in informing the optimization design of the anti-icing cavity structure.

The most widely used methods for reliability sensitivity analysis include the Monte Carlo method [15], first-order second-moment method [16], and response surface method [17, 18]. A major drawback of the first-order second-moment method is that the estimation error in a nonlinear situation is quite large, while the Monte Carlo method places less demand on the expression of the limit state equation but more demand on the sampling number to ensure calculation accuracy. The Fluent software [19] is used to simulate the performance of an anti-icing cavity, typically taking about half an hour on a 3.20 GHz Intel Core i5-3470 CPU with 4 GB NVIDIA GeForce 605 memory. This long calculation time makes use of the Monte Carlo method to conduct the analysis somewhat infeasible. When using the response surface method, the implicit performance function should first be fitted into an explicit expression; then, an analysis is performed based on this explicit expression. However, the traditional polynomial response surface method can only meet the accuracy requirements using multiple iterations, and the computational cost remains significant. The stochastic response surface method adopts the Hermite polynomial chaos expansion model and its output to fit the performance function expression without requiring iterative computations [20]. Accordingly, this method can be used to improve the solution efficiency of an anti-icing cavity functional reliability sensitivity analysis. In order to insure sufficient fitting accuracy, the traditional response surface method usually adopts a weighting strategy by increasing the weight factors of the sample points that have a smaller value for the limit state function in order to approach the actual limit state equation on more preferable terms [21, 22]. This paper therefore introduces the idea of weighting into the stochastic response surface method to improve the fitting accuracy of the anti-icing cavity performance function.

With the objective of analysing the anti-icing cavity of an airfoil thermal anti-icing system, the computational fluid mechanics software package Fluent was used in this study to simulate the anti-icing cavity and obtain the effective availability of anti-icing hot air. The critical anti-icing thermal efficiency was defined as the failure criterion, and an expression for the explicit performance function was obtained by the weighted stochastic response surface method. Finally, the Monte Carlo method was used to calculate the sensitivity values of the structure parameters based on the results of the previous steps.

The remainder of this paper is organized as follows. The basic principle of the weighted stochastic response surface method and reliability sensitivity analysis is introduced in Section 2. The performance reliability sensitivity analysis of the anti-icing cavity thermal efficiency is provided in Section 3, and conclusions are presented in Section 4.

2. Numerical Methods

2.1. Weighted Stochastic Response Surface Method. The stochastic response surface method was originally proposed by Isukapalli et al. [23, 24] as an evolution of the classical response surface method during their study on the uncertainty of environmental and economic systems. The first step of the stochastic response method is used to express a normal random variable δ_i as a function of a standard normal random variable ζ_i, using the following conversion equation:

$$\delta_i = \mu_i + \sigma_i \zeta_i, \tag{1}$$

where μ_i and σ_i are the mean value and standard deviation of the normal variable δ_i, respectively.

On this basis, the output response can be converted into a Hermite stochastic polynomial expansion model that contains mere standard normal stochastic variables as follows:

$$\begin{aligned} y(\xi_i) = {} & a_0\Gamma_0 + \sum_{i_1=1}^{n} a_{i_1}\Gamma_1\left(\xi_{i_1}\right) + \sum_{i_1=1}^{n}\sum_{i_2=1}^{i_1} a_{i_1 i_2}\Gamma_2\left(\xi_{i_1},\xi_{i_2}\right) \\ & + \sum_{i_1=1}^{n}\sum_{i_2=1}^{i_1}\sum_{i_3=1}^{i_2} a_{i_1 i_2 i_3}\Gamma_3\left(\xi_{i_1},\xi_{i_2},\xi_{i_3}\right)+\cdots \\ & + \sum_{i_1=1}^{n}\sum_{i_2=1}^{i_1}\sum_{i_3=1}^{i_2}\cdots\sum_{i_n=1}^{i_{n-1}} a_{i_1 i_2 i_3,\ldots,i_n}\Gamma_n\left(\xi_{i_1},\xi_{i_2},\xi_{i_3},\cdots,\xi_{i_n}\right), \end{aligned} \tag{2}$$

where a_0, a_{i_1}, $a_{i_1 i_2}$, $a_{i_1 i_2 i_3}$, and $a_{i_1 i_2 i_3,\ldots,i_n}$ are undetermined coefficients, n is the number of stochastic variables, and $\Gamma_n(\xi_{i_1},\xi_{i_2},\xi_{i_3},\cdots,\xi_{i_n})$ is an n-order polynomial, defined as

$$\Gamma_n\left(\xi_{i_1},\xi_{i_2},\xi_{i_3},\cdots,\xi_{i_n}\right) = (-1)^n e^{(1/2)\xi^T\xi} \frac{\partial^n}{\partial\xi_{i_1}\partial\xi_{i_2}\cdots\partial\xi_{i_n}} e^{-(1/2)\xi^T\xi}. \tag{3}$$

From equation (2), it can be seen that when the number of stochastic variables of the output stochastic response is n, the computational equation for the number of terms in the p-order Hermite random polynomial expansion can be expressed as

$$N = \frac{(n+p)!}{n!p!}. \tag{4}$$

We can then obtain the response function expression $y(\xi_i)$ once $\Gamma_n(\xi_{i_1},\xi_{i_2},\xi_{i_3},\cdots,\xi_{i_n})$ is estimated. For convenience of description, the second-order expansion for two stochastic variables is shown as follows:

$$\begin{aligned} y(\xi_1,\xi_2) = {} & a_0 + a_1\xi_1 + a_2\xi_2 + a_3\left(\xi_1^2 - 1\right) \\ & + a_4\left(\xi_2^2 - 1\right) + a_5\xi_1\xi_2, \end{aligned} \tag{5}$$

where six undetermined coefficients $a_i (i = 0, 1, 2, \cdots, 5)$ are required for the second-order expansion model y_2.

Solving for the undetermined coefficients a_i is the key step in the stochastic response surface method. At present, the most common methods for doing so are the probabilistic collocation method, modified probabilistic collocation method, and efficient regression method. Among these methods, the efficient regression method is able to obtain the most stable results: when the input variables are $\xi_{1,i}$ and $\xi_{2,i}$, equation (5) can be transformed into

$$\begin{aligned} y(\xi_{1,i},\xi_{2,i}) = {} & a_0 + a_1\xi_{1,i} + a_2\xi_{2,i} + a_3\left(\xi_{1,i}^2 - 1\right) \\ & + a_4\left(\xi_{2,i}^2 - 1\right) + a_5\xi_{1,i}\xi_{2,i}. \end{aligned} \tag{6}$$

In order to obtain the six undetermined coefficients in equation (6), proper sample points are chosen, yielding the combined form of the sample points as

$$(\xi_{1,1}, \xi_{2,1}), (\xi_{1,2}, \xi_{2,2}), \dots, (\xi_{1,m}, \xi_{2,m}). \tag{7}$$

The values of $\xi_{1,i}$ and $\xi_{2,i}$ in equation (7) are the roots of the $p+1$-order Hermite polynomial, and equation (6) is the expansion model of the second-order Hermite polynomial; therefore, the roots $(0, \sqrt{3}, \text{and} -\sqrt{3})$ of the third-order Hermite polynomial can be taken as the values of the input variables $\xi_{1,i}$ and $\xi_{2,i}$. The number of collocation points available is $N_a = (p+1)^n$, so there are nine potential sample points. When there are more sample variables, the available collocation points are much more numerous than the undetermined coefficients, so the number of sample points is usually selected as twice as the number of undetermined coefficients.

The sample points chosen using the above method are standard normal variables, so they need to be transformed into original random variables by equation (1) before calculation; then, the corresponding authentic performance function matrix $\bar{y}$ of the sample points can be calculated, and finally the six undetermined coefficients a_i can be obtained by solving this system of linear equations using the least square method, i.e.,

$$a = \left(B^T B\right)^{-1} B^T \bar{y}, \tag{8}$$

where B, which is a 9×6 matrix composed of nine sample points, and $\bar{y}$ are given as follows, respectively,

$$B = \begin{bmatrix} 1 & \delta_{11} & \delta_{12} & \left(\delta_{11}^2 - 1\right) & \left(\delta_{12}^2 - 1\right) & \delta_{11}\delta_{12} \\ 1 & \delta_{21} & \delta_{22} & \left(\delta_{21}^2 - 1\right) & \left(\delta_{22}^2 - 1\right) & \delta_{21}\delta_{22} \\ \vdots & \vdots & \vdots & \vdots & \vdots & \vdots \\ 1 & \delta_{91} & \delta_{92} & \left(\delta_{91}^2 - 1\right) & \left(\delta_{92}^2 - 1\right) & \delta_{91}\delta_{92} \end{bmatrix},$$
$$\bar{y} = \{y(\delta_1), y(\delta_2), \cdots, y(\delta_9)\}^T. \tag{9}$$

To further improve the fitting accuracy of the stochastic response surface method, the concept of weighted regression is proposed to fit the stochastic response surface method by adopting the weighted least square method. This approach has the effect of increasing the weight factors w_i of the sample points with smaller values of $|y(\delta_i)|$ to cause them to play more important roles, thus making $\bar{y}(\delta) = 0$ close to $y(\delta) = 0$. The weighted regression form of coefficient a is expressed as

$$a = \left(B^T w B\right)^{-1} B^T w \bar{y}, \tag{10}$$

where $w = \mathrm{diag}(w_i)$ is a weighting matrix.

The value of weight w_i depends on the gap between the sample points and the limit state function $y(\delta) = 0$, determined as follows:

$$w_i = \frac{\min_{i=1}^{9} |y(\delta_i)|}{|y(\delta_i)|}. \tag{11}$$

After obtaining the coefficient a_i, the second-order explicit response surface function can be obtained. Thus, the required amount of simulation computation is greatly reduced, and the reliability sensitivity can be effectively calculated by the Monte Carlo method [15].

2.2. Reliability Sensitivity Analysis. Reliability sensitivity reflects the influence of the change in stochastic variables on system reliability, providing guidance for structural optimization design [25, 26]. The weighted stochastic response surface method introduced in Section 2.1 can be used to obtain an explicit performance function, and the Monte Carlo method can then be adopted to provide a reliability sensitivity analysis without requiring the use of the Fluent software package, significantly simplifying the computation process.

The explicit performance function $y(\delta)$ is generated by the weighted stochastic response surface method, where $\delta = \{\delta_1, \delta_2, \cdots, \delta_n\}$ is a basic random variable that follows the normal distribution, so the failure possibility P_f can thus be expressed as

$$P_f = P(y(\delta) \le 0) = \int_\Omega f(\delta) d\delta, \tag{12}$$

where $f(\delta)$ is the joint probability density function and $\Omega = \{\delta | y(\delta) \le 0\}$ is the failure domain.

Reliability sensitivity is defined as the partial derivative of P_f with respect to the distribution parameter $\delta = \{\delta_1, \delta_2, \cdots, \delta_n\}$, and the reliability sensitivity of the failure probability P_f to the mean value μ_i can be obtained by

$$\frac{\partial P_f}{\partial \mu_i} = \int_\Omega \frac{\partial f(\delta)}{\partial \mu_i} d\delta, \tag{13}$$

describing the influence of the mean value of the basic variable on the failure probability, which can be expressed as

$$\frac{\partial P_f}{\partial \mu_i} = P_f E\left[\frac{\partial f(\delta)}{\partial \mu_i} \frac{1}{y(\delta)}\right]_\Omega = P_f E\left[\frac{\delta_i}{\sigma_i}\right]_\Omega. \tag{14}$$

The sensibility of failure probability P_f to the standard deviation is defined as

$$\frac{\partial P_f}{\partial \sigma_i} = \int_\Omega \frac{\partial f(\delta)}{\partial \sigma_i} d\delta, \tag{15}$$

describing the influence of the standard deviation of the basic variable on the failure probability, which can be expressed as

$$\frac{\partial P_f}{\partial \sigma_i} = P_f E\left[\frac{\partial f(\delta)}{\partial \sigma_i} \frac{1}{y(\delta)}\right]_\Omega = P_f E\left[\frac{\delta_i}{\mu_i}\right]_\Omega. \tag{16}$$

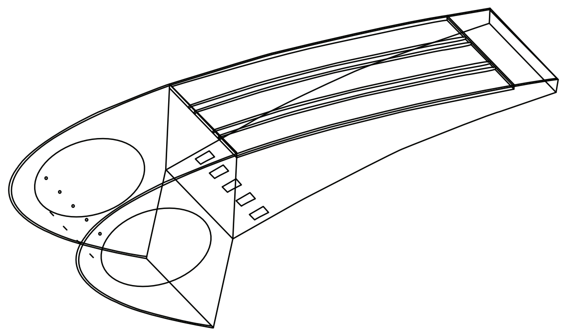

(a) General outline of the anti-icing cavity

(b) Structure of the double skin

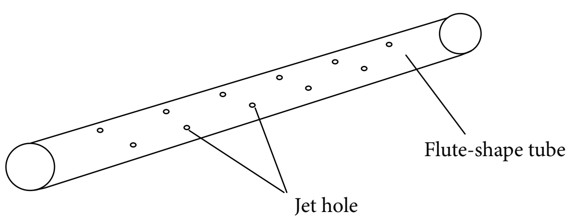

(c) Flute

Figure 1: Sketches of the subject anti-icing cavity.

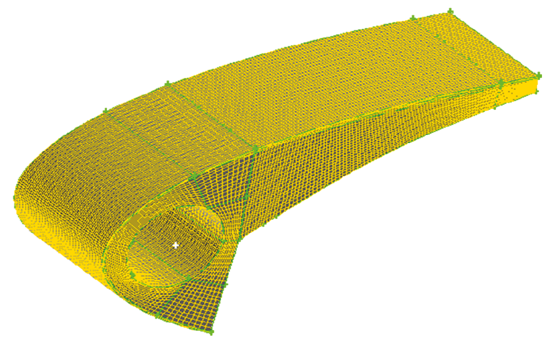

Figure 2: Overall anti-icing cavity grid model.

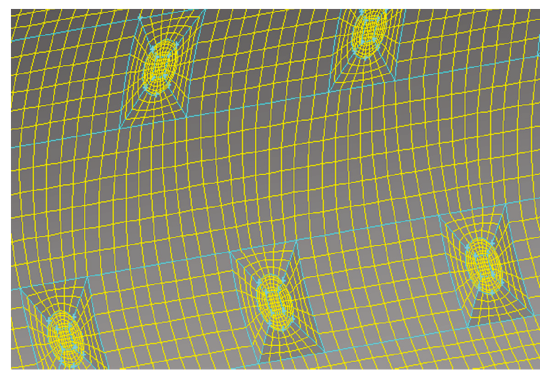

Figure 3: Grid model detail around jet holes.

3. Performance Reliability Sensitivity Analysis of Anti-Icing Cavity Thermal Efficiency

3.1. Calculation Model. The anti-icing cavity structure considered in this study is shown in Figure 1, representing a direct injection double-skin anti-icing cavity. The 3D model of the subject anti-icing cavity was built using Gambit [27]. The thickness of the double skin is 1.6 mm, the channel height of the double skin is 3 mm, the outside diameter of the flute is 34 mm, the distance between the cavity centre and the edge of the wing is 37 mm, and the two arrays of the 2 mm circular jet holes are staggered along the topside of the flute at a pitch of 25 mm and angles of $\pm 15^{\circ}$. The hot air transmitted from the engine compressor flows through a pipe into the flute inside the slat on the leading edge of the wing where it is jetted out through the jet holes onto the internal surface of the front anti-icing cavity to heat the airfoil skin, after which the hot gas flows through the channel inside the double skin and towards the back anti-icing cavity, where it is then emitted from the vent in the back cavity.

3.2. Numerical Simulation. The 3D thermal anti-icing cavity was modelled with the Gambit preprocessing software. In order to increase computational accuracy, structured grids were generated in the model using meshes densified around the jet holes and boundary layer meshes near the front anti-icing wall. Because skin temperature is a significant parameter and the skin thickness is only 1.6 mm, the meshes were densified and the skin grid height was set as 0.16 mm. Overall, the anti-icing cavity model consists of about 630,000 grids. The anti-icing cavity mesh model is shown in Figure 2, and the mesh model around the jet holes is shown in Figure 3. Cavity flow and heat transfer were simulated using Fluent and the energy equation. This study selected the proper S-A turbulence model, which is a good fit for impinging jet surface computations, and set the discretization scheme as a second-order upwind scheme.

For boundary conditions, each jet hole was set as a pressure inlet with a pressure of 0.2 MPa, the hot gas temperature was set at 473.15 K, the exit temperature was set the same as the environment temperature at 263.15 K, the baffles on both sides were set as symmetric boundaries, and the anti-icing cavity external skin surface was set as the convection boundary condition, for which the convective heat transfer coefficient reflects the external flow field velocity. Specific boundary condition types are presented in Table 1.

3.3. Assessment of Anti-Icing Cavity Heat Transfer Performance. The Fluent simulation of gas flow converged after about 5000 iterations. The distribution of the external skin surface temperature after convergence is shown in Figure 4, in which it can be seen that the temperature reaches its maximum value around the leading edge stagnation point, then decreases along the chord before reaching its minimum value at the end of the anti-icing cavity, changing a total of about 60 K. The effect of the double-skin channel can be observed in the difference in skin temperature on the upper

Table 1: Boundary condition types.

Boundary condition	Type
Jet hole	Pressure inlet
Export of the flow field	Pressure outlet
Outside skin surface	Convection wall
Inside skin surface	Coupled wall
Wall flute	Fixed temperature wall
Back shield	Adiabatic wall
Both sides of the baffle	Symmetry

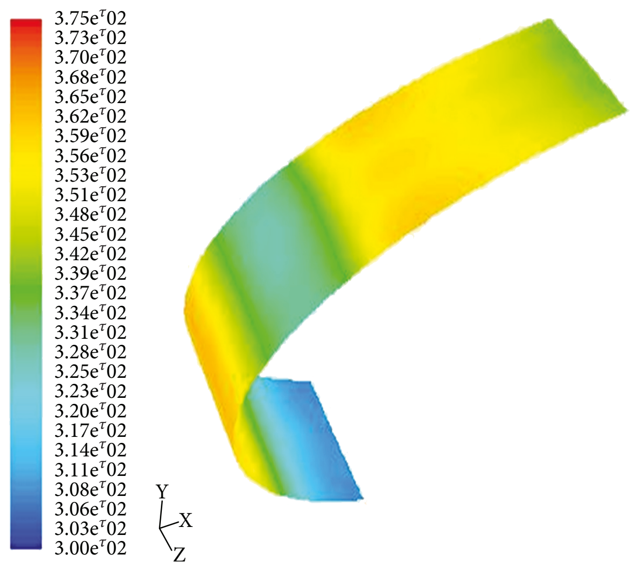

Contours of total temperature (k)

Figure 4: Temperature nephogram of the wing skin surface.

and lower surfaces in the anti-icing area: the upper surface exhibits an obvious rising trend prior to entering the double-skin channel and a decreasing trend along the chord, so the temperature on the upper surface is higher than that on the lower surface. The more complete contact between the air flow and the skin in the double-skin channel clearly provides superior heat transfer performance.

In order to verify the accuracy of their simulation, which was constructed using an approach similar to that in the current study, [28] built a test platform with which to evaluate the anti-icing performance of a certain type of hot air wing anti-icing cavity structure, and these test results were found to be consistent with their numerical simulation results.

To intuitively reflect the anti-icing ability of the anti-icing cavity, this study introduces the concept of anti-icing efficiency η to describe the percentage of hot gas energy provided by the system to warm the anti-icing surface, expressed as

$$\eta = \frac{T_{\text{inlet}} - T_{\text{outlet}}}{T_{\text{inlet}} - T_{\text{wall}}}, \quad (17)$$

where T_{inlet} and T_{outlet} are the gas supply temperature and exhaust temperature of the anti-icing system, respectively, and T_{wall} is the average temperature of the anti-icing area. Low anti-icing efficiency will lead to a marked increase in the engine air supply required to provide sufficient anti-icing performance, not only resulting in fuel waste but also increasing the load on the engine, which is harmful to its short- and long-term performance. Therefore, anti-icing efficiency can be an important way to assess the effectiveness of anti-icing cavity design.

3.4. Reliability Sensitivity Analysis. The four most important parameters influencing anti-icing efficiency, the distance between the centre of the flute and the skin H, the height of the double-skin channel h, the jet hole diameter d, and the jet hole angle θ, were chosen as stochastic variables to analyse the system reliability sensitivity. These variables are normal random variables that are mutually independent of each other.

An appropriate test point for the four subject parameters was selected using the stochastic response surface method. Through equation (4), 15 unknown coefficients need to be solved when performing the second-order Hermite stochastic polynomial expansion. There are 3^4 optional test points, from which twice the number of unknown coefficients (i.e., 30 in this case) was selected by the efficient regression method and inserted into the Fluent simulation.

When studying the problems of anti-icing system performance reliability, the failure criteria must first be defined. For the subject hot air anti-icing system, this study selected the critical anti-icing efficiency η^* as the failure criteria of the anti-icing system. The critical anti-icing efficiency was identified by considering the maximum anti-icing hot air supply provided by the engine that meets the dynamic conditions and anti-icing hot air demand. Once the anti-icing efficiency η is below the critical anti-icing efficiency η^*, the anti-icing system is regarded as failed. Accordingly, the anti-icing system performance function is given by

$$y = \eta - \eta^*, \quad (18)$$

where η is an implicit function of (H, h, d, θ), which must be computed using the Fluent software package at the test points.

By selecting the critical hot gas anti-icing efficiency value η^* as 39% and the variation coefficient of the random variables as 0.1, the explicit expression of the performance function can be fitted by the weighted stochastic response surface method, and the reliability sensitivity can then be analysed by the Monte Carlo method. The anti-icing cavity function reliability sensitivity was thus calculated under different entrance temperatures with the results presented in Table 2, where μ_H, μ_h, μ_d, and μ_θ are the average values of H, h, d, and θ, respectively, and σ_H, σ_h, σ_d, and σ_θ are the standard deviations of H, h, d, and θ, respectively.

As can be observed in Table 2, the sensitivity analysis results indicate that an increase in the standard deviations of the angles between the jet holes and the horizontal plane will lead to a decrease in failure probability; P_f increases with the increase in μ_H, σ_H, μ_h, σ_h, μ_d, σ_d, and μ_θ; the sensitivities

Table 2: Anti-icing cavity function reliability sensitivity under different entrance temperatures.

	Temperature (K) 473.15	483.15	493.15
$\frac{\partial \widehat{P}_f}{\partial \mu_H}$	0.0003741	0.0003281	0.0003041
$\frac{\partial \widehat{P}_f}{\partial \sigma_H}$	0.0002142	0.0002014	0.0001943
$\frac{\partial \widehat{P}_f}{\partial \mu_h}$	0.0112556	0.0105842	0.0102556
$\frac{\partial \widehat{P}_f}{\partial \sigma_h}$	0.0179093	0.0156254	0.0149093
$\frac{\partial \widehat{P}_f}{\partial \mu_d}$	0.026811	0.025322	0.023811
$\frac{\partial \widehat{P}_f}{\partial \sigma_d}$	0.0704587	0.0650598	0.0614587
$\frac{\partial \widehat{P}_f}{\partial \mu_\theta}$	0.0001327	0.0001112	0.0000927
$\frac{\partial \widehat{P}_f}{\partial \sigma_\theta}$	-0.0006281	-0.0005549	-0.0004881

of μ_h, σ_h, μ_d, and σ_h are relatively larger than those of the other factors, indicating that they are the main factors influencing the functional reliability of the anti-icing cavity. Accordingly, reducing the double-skin channel height and the average diameter and the standard deviation of the jet holes will increase the functional reliability of the system, and the functional reliability sensitivity of the anti-icing cavity decreases with the increase in the hot air temperature at the entrance.

4. Conclusions

This study conducted a functional reliability sensitivity analysis of an aircraft wing anti-icing cavity. The accuracy and computational efficiency problems associated with the functional reliability sensitivity analysis of an anti-icing cavity were solved using the CFD simulation software, the weighted stochastic response surface method, and the Monte Carlo method. First, the functional efficiency of an anti-icing cavity was calculated using a Fluent simulation; then, an anti-icing function reliability sensibility analysis model was constructed, the explicit expression was fitted using the weighted stochastic response surface method, and finally the reliability sensitivities of the anti-icing cavity structural parameters were calculated.

The calculation results indicate that the double-skin channel height and jet hole diameter are the key structural parameters influencing the functional reliability of an anti-icing cavity, suggesting that the reliability of an aircraft wing anti-icing system can be improved by the adjustment of the double-skin channel height and jet hole diameter. This method can be accordingly applied to different anti-icing system designs to determine the parameters that provide the optimal functionality, improving aircraft safety and performance in icy conditions.

Data Availability

In the manuscript 7851260 titled "Structural Parameter Sensitivity Analysis of an Aircraft Anti-Icing Cavity Based on Thermal Efficiency," all data analysed during this study are included in this manuscript. Therefore, there is no additional data available.

Conflicts of Interest

The authors declare that they have no conflicts of interest.

Acknowledgments

The authors gratefully acknowledge the support of the China Scholarship Council, the Top International University Visiting Program for Outstanding Young Scholars of Northwestern Polytechnical University, the Fundamental Research Fund for the Central Universities (NPU-FFR-3102015BJ(II) JL04), and the Natural Science Foundation of Shaanxi Province (2016JQ5109).

References

[1] F. Zhang, W. W. Deng, H. Nan, L. Zhang, and Z. Huang, "Reliability analysis of bleed air anti-icing system based on subset simulation method," *Applied Thermal Engineering*, vol. 115, pp. 17–21, 2017.

[2] Z. Li, H. J. Xu, Y. Xue, and X. L. Wang, "Research on flight safety effect mechanism and protection for aircraft icing," *Flight Dynamics*, vol. 34, no. 4, pp. 10–14, 2016.

[3] C. Zilio and L. Patricelli, "Aircraft anti-ice system: evaluation of system performance with a new time dependent mathematical model," *Applied Thermal Engineering*, vol. 63, no. 1, pp. 40–51, 2014.

[4] H. H. Li and M. Zhou, "Engineering application of icing detection technique and anti-icing and deicing system on aircraft," *Advances in Aeronautical Science and Engineering*, vol. 1, no. 2, pp. 112–115, 2010.

[5] S. N. Chang, B. Yang, M. Y. Leng, Y. Y. Zhao, and M. Y. Liu, "Study on bleed air anti-icing system of aircraft," *Journal of Aerospace Power*, vol. 32, no. 5, pp. 1025–1034, 2017.

[6] X. Q. Bu, J. Yu, and G. P. Lin, "Investigation of the design of wing thermal anti-icing system," *Journal of Beijing University of Aeronautics and Astronautics*, vol. 36, no. 8, pp. 927–930, 2010.

[7] F. Zhang, H. J. Yao, H. Nan, and C. C. Lu, "Importance measure of aircraft anti-icing cavity structure parameters," *Journal of traffic and transportation Engineering*, vol. 15, no. 3, pp. 85–91, 2015.

[8] J. Z. Zhang, T. Guan, and Y. Shan, "Influence of piccolo tube parameters on temperature distribution on hot air anti-icing concave surface," *Journal of Nanjing University of Aeronautics & Astronautics*, vol. 49, no. 5, pp. 669–675, 2017.

[9] H. J. Yao, Y. S. Liu, F. Zhang, and H. Nan, "Numerical simulation of impact of structure parameter on hot air anti-icing system performance," *Aeronautical Manufacturing Technology*, vol. 15, pp. 46–49, 2015.

[10] L. Peng, X. Q. Bu, G. P. Lin, W. T. Ma, and K. Zhao, "Influence of the structural parameters on thermal performance of the hot air anti-icing system," *ACTA Aerodynamica Sinica*, vol. 32, no. 6, pp. 848–853, 2014.

[11] F. Zhang, K. L. Luo, W. H. Zhai, S. Tan, and Y. Wang, "Non-probabilistic parameter sensitivity analysis for structures based on ellipsoidal model," *Advances in Mechanical Engineering*, vol. 10, no. 8, p. 7, 2018.

[12] T. V. Steenkiste, J. Herten, I. Couckuyt, and T. Dhaene, "Sequential sensitivity analysis of expensive black-box simulators with metamodelling," *Applied Mathematical Modelling*, vol. 61, pp. 668–681, 2018.

[13] S. Sankaran, J. D. Humphrey, and A. L. Marsden, "An efficient framework for optimization and parameter sensitivity analysis in arterial growth and remodeling computations," *Computer Methods in Applied Mechanics and Engineering*, vol. 256, pp. 200–210, 2013.

[14] F. Zhang, Z. Z. Lu, L. J. Cui, and S. Shufang, "Reliability sensitivity algorithm based on stratified importance sampling method for multiple failure modes systems," *Chinese Journal of Aeronautics*, vol. 23, no. 6, pp. 660–669, 2010.

[15] G. X. Chen, C. X. Cui, Z. Y. Fu, and M. M. Jiang, "Reliability sensitivity analysis of underground silo based on Monte-Carlo stochastic finite element method," *Journal of Henan University of Technology*, vol. 38, no. 4, pp. 86–90, 2017.

[16] S. Zheng, *Modeling and Sensitivity Analysis of Movement Function Reliability of Deployable Mechanism of Folded Wings*, Zhejiang Sci-Tech University, Hangzhou, 2017.

[17] L. Wang, *Study on Reliability and Sensitivity of Metal Structure of Overhead Travelling Crane Based on Response Surface Method*, Taiyuan University of Science and Technology, Taiyuan, 2016.

[18] P. L. Xiang, Y. H. Lu, L. Y. Dang, Z. Feng, and J. Zeng, "Method comparison research of reliability parametric sensitivity analysis for high speed train carbody," *Journal of Dalian Jiaotong University*, vol. 38, no. 5, pp. 15–21, 2017.

[19] T. Li, J. Y. Zhang, Z. J. Li, and W. H. Zhang, "Co-simulation on fluid-structure interaction of high-speed train based on Fluent and Simpack," *Chinese Journal of Computational Mechanics*, vol. 29, no. 5, pp. 675–680, 2012.

[20] F. Wang and H. Li, "Stochastic response surface method for reliability problems involving correlated multivariates with non-Gaussian dependence structure: analysis under incomplete probability information," *Computers and Geotechnics*, vol. 89, pp. 22–32, 2017.

[21] U. Alibrandi, "A response surface method for stochastic dynamic analysis," *Reliability Engineering & System Safety*, vol. 126, pp. 44–53, 2014.

[22] R. Chutia, S. Mananta, and D. Datta, "Uncertainty modelling of atmospheric dispersion by stochastic response surface method under aleatory and epistemic uncertainties," *Sadhana*, vol. 39, no. 2, pp. 467–485, 2014.

[23] S. S. Isukapalli, A. Roy, and P. G. Georgopoulos, "Stochastic response surface methods (SRSMs) for uncertainty propagation: application to environmental and biological systems," *Risk Analysis*, vol. 18, no. 3, pp. 351–363, 1998.

[24] S. S. Isukapalli, A. Roy, and P. G. Georgopoulos, "Efficient sensitivity/uncertainty analysis using the combined stochastic response surface method and automated differentiation: application to environmental and biological systems," *Risk Analysis.*, vol. 20, no. 5, pp. 591–602, 2000.

[25] I. Papaioannou, K. Breitung, and D. Straub, "Reliability sensitivity estimation with sequential importance sampling," *Structural Safety*, vol. 75, pp. 24–34, 2018.

[26] H. A. Jensen, F. Mayorga, and C. Papadimitriou, "Reliability sensitivity analysis of stochastic finite element models," *Computer Methods in Applied Mechanics and Engineering*, vol. 296, pp. 327–351, 2015.

[27] B. Xiao, A. G. Shi, and X. Wang, "Fully appendage modeling of ships based on GAMBIT," *Ship Engineering*, vol. 32, pp. 32–36, 2010.

[28] H. J. Yao, *Function Reliability Analysis and Optimal Design of the Wing Hot-Air Anti-Icing Cavity*, Northwestern Polytechnical University, Xi'an, 2014.